Efficient Tm:YAG and Tm:LuAG lasers pumped by 681-nm tapered diodes

ERSEN BEYATLI,[1] BERND SUMPF[2], GÖTZ ERBERT[2], UMIT DEMIRBAS[3,4,*]

[1]*Department of Electrical-Electronics Engineering, Recep Tayyip Erdogan University, Rize, 53100, Turkey*
[2]*Ferdinand-Braun-Institut, Leibniz Institut für Höchstfrequenztechnik, D-12489 Berlin, Germany*
[3]*Laser Technology Laboratory, Department of Electrical and Electronics Engineering, Antalya Bilim University, 07190 Antalya, Turkey*
[4]*Center for Free-Electron Laser Science, Deutsches Elektronen Synchroton (DESY), Hamburg, Germany*
**Corresponding author: umit79@alum.mit.edu*

Abstract

In this paper, we present highly-efficient continuous-wave (cw) laser operation of Tm:YAG and Tm:LuAG lasers pumped by high-brightness red tapered diodes. The single-emitter tapered diode lasers (TDLs) provide up to 1-W of pump power around 680 nm. By adjusting the operation temperature of the TDL, the pump central wavelength could be matched to the strong absorption peak of Tm^{3+} ions in this region ($^3H_6 \rightarrow {}^3F_3$ excitation). This absorption peak is around 3-fold stronger than the usually employed 785 nm transition ($^3H_6 \rightarrow {}^3H_4$) . In the cw laser experiments, we have achieved slope efficiencies exceeding 55% at room temperature, which is far above the stokes limited slope efficiency (34%), indicating presence of strong two-for-one cross-relaxation process. Pumping with high-brightness tapered diode lasers further facilitated usage of smaller pump spots (enabling quite low lasing thresholds) and generation of near-diffraction limited output beam profiles from standard z-type cavities. To the best of our knowledge, this is the first report of diode pumping of Tm-doped solid-state lasers around 680 nm, as well as the first usage of TDLs as pump sources in Tm-doped laser systems.

1. Introduction

All-solid-state, diode-pumped eye-safe lasers working in the 2 μm region are favorable for many applications including medicine, laser radar, material processing, optical frequency conversion, gas sensing and pumping of Ho-based and Cr-based lasers (e.g. Cr:ZnSe) [1-4]. Tm-doped crystals such as Tm:YAG and Tm:LuAG are among the commonly employed laser gain media for this purpose [5-9]. Thulium-based laser systems are usually pumped by laser diodes [10-14] or Ti:Sapphire lasers [15] operating around 785 nm (exact absorption peak position is host dependent: [16-18]). For this pump wavelength, the corresponding stokes limit for laser slope efficiency is then about 39% (quantum defect limited slope efficiency). On the other hand, for highly-doped thulium-samples (Tm^{+3}-doping>3%), the two-for-one cross-relaxation process enables extraction of laser efficiencies exceeding stokes limit. As an example, a slope efficiency of 59% has been reported from a 785 nm Ti:Sapphire pumped room temperature Tm:YAG laser (12% Tm-doping), indicating a cross-relaxation efficiency of around 1.5 (also known as photon quantum efficiency: one 785 nm pump photon generating 1.5 laser photons around 2 μm) [15]. A 786-nm diode pumped 4% Tm-doped Tm:YAG ceramic laser reported slope efficiencies up to 65% at a heatsink temperature of 8 °C (cross-relaxation efficiency:1.67) [19]. A slope efficiency above 70% has also been shown from a 792 nm fiber coupled diode-pumped Tm:CaF2 laser operating around 1917 nm [20]. Note that, due to the relatively low brightness of diode pump sources, usually these high slope efficiencies could be obtained only from compact (5-10 cm) and simple two-mirror laser cavities, which typically also produce multimode laser output beams. Unfortunately, these constraints create strong boundaries for mode-locking studies; limiting progress in achieving simple femtosecond diode pumped Tm-based laser systems.

As an alternative pumping approach, in-band pumping of Thulium-lasers in the 1.5-1.8 μm region is an attractive option [21-25]. The absorption band of thulium ion around this spectral region is about two-fold stronger than the one around 785 nm. On top of that, pumping at a wavelength very close to the lasing transition, reduces quantum defect and potentially enables construction of lasers/amplifiers with very high slope efficiencies. Moreover, while exciting Tm-based gain media in the 1.5-1.8 μm region, laser efficiency is not based on the two-for-one cross-relaxation process. Hence, one can freely optimize the Tm-concentration of

the laser gain media for minimization of thermal effects, which could be a great advantage in power scaling studies. On the other hand, laser diodes in this spectral region is not as progressed as their 785 nm counterparts yet (i.e.: output powers available from 785 nm single-mode laser diodes are an order of magnitude higher compared to those in the 1.5-1.8 μm region) [26, 27]. Hence, in most of the in band pumping studies, other solid-state lasers have been used as pump sources: Nd:YAG laser pumped Co:MgF2 laser at 1682 nm [22], Raman-shifted Er-fiber laser at 1678 nm [23] and 1693 nm [28], Er:YAG ceramic lasers at 1617 nm [24], and Er^{3+}:Yb^{3+} fiber master oscillator power amplifier at 1611 nm [25]. In these studies, slope efficiencies of 42% using 5% Tm-doped Tm:YLF [24], 50% using 1.5% Tm-doped Tm:YLF [24], 59% using 5.2% Tm-, 0.5% Ho-doped Tm,Ho:YLF [22], 60% using Tm:CGA [28], and 62.3% using 4% Tm-doped Tm:YAG ceramic [24] were reported. As an extreme case, a slope efficiency above 90% has been realized from a 1908 nm Tm:fiber pumped Tm:fiber laser operating at 2005 nm [29]. Note that, the high brightness of these laser based pump sources also enabled demonstration of Kerr-lens mode-locking (KLM) in a Tm^{+3}-doped solid-sate laser to the first time (Tm^{+3}:Sc_2O_3, 47% efficiency in mode-locked regime [25]). On the other hand, these laser based pump sources are relatively high-cost, complex and bulky, and lack the advantages of direct diode pumping. Troshin et al. demonstrated first diode pumping of Tm-systems in this spectral region, using a 2-W fiber-coupled diode laser operating at 1590 nm[21]. However, the reported slope efficiency was only 28%, most probably due to the limited brightness of the diode source [21]. Hence, further progress in spectral brightness of 1.5-1.8 μm diodes is required for their efficient usage in pumping of Tm-systems.

As the third approach, Stoneman et al. proposed pumping of Tm-based lasers around 680 nm [30]. The absorption bands around this spectral region posses the largest absorption coefficient in Tm-systems [17, 30]. Compared to 785 nm pumping, the absorption coefficient is around 3-fold stronger, and hence usage of the 681 nm line facilitates utilization of shorter Tm-crystals, which is attractive for several different reasons. First of all, in quais-3-level laser gain media such as Tm-based systems, usage of shorter crystals reduces self-absorption losses especially on the short wavelength side of the tuning range, which could then extend the cw tuning range and provide shorter pulses in mode-locked regime [30]. In addition, 681 nm pumping also enables usage of thinner crystals in slab and thin-disk geometries, which has advantages in power scaling (decreasing thickness reinforces heat extraction) [14, 31]. Furthermore, in a recent study, Cho et al. showed that minimization of self-absorption losses suppresses self-Q-switching tendency in Tm:YAG lasers, and facilitates generation of clean cw mode-locked pulses via KLM [32]. Moreover, for a fixed crystal doping level, pumping at a wavelength with stronger absorption coefficient, creates a more densely excited gain medium, which could potentially increase the effectiveness of cross-relaxation process. Hence, with 681-nm excitation, a lower Tm^{+3} doping might be sufficient for the cross-relaxation to become effective. As a drawback, for this pumping scheme, the stokes limited slope efficiency reduces to 34%; thus, considering the two-for-one cross-relaxation mechanism, the maximum slope efficiency that could be achieved is limited to 68%. Another possible disadvantage is the increased role of thermal effects due to the larger absorption coefficients, which will require special care in laser design. In their early work, Stoneman et al. used a Ti:Sapphire laser operating at 681 nm to pump a Tm:YAG crystal, but the obtained slope efficiency was only around 35%, indicating a weak cross-relaxation process [30]. Matos et al. pumped a 9.5%-Yb- and 1.15% Tm-doped Yb:Tm:YLF crystal simultaneously with 685 nm and 980 nm diodes, and obtained a slope efficiency of 10% only [33]. Due to the inefficient side-pumping geometry, lasing could not be achieved while pumping the system only with the 5W 685-nm multimode diode laser [33].

In this work, to the best of our knowledge, we present: (i) first diode pumping of Tm-doped gain medium around 681-nm and (ii) the first implementation of high-brightness tapered diode lasers as pump sources for Tm-based solid-state lasers. Tm:YAG and Tm:LuAG gain medium have been chosen for the test. The TDL delivered up to 1 W of output power with a tunable optical spectrum cantered around 680 nm that could be matched to the absorption peak of Tm^{+3} ions in different hosts. In the cw laser experiments, we have obtained up to 340 mW and 295 mW of output powers and acquired slope efficiencies of 55.5% and 51% at room temperature from Tm:YAG and Tm:LuAG lasers, respectively. These efficiency values are similar to what could be achieved from diode-pumped 785 nm systems, showing the effectiveness of 681 nm pumping route. Moreover, due to the high brightness of the tapered diode laser that is used in this study, we could achieve near-diffraction limited output beam profiles using a standard z-type cavity, providing great advantages in future mode-locking studies compared to low-brightness multimode diode pumped systems.

The paper is organized as follows: Section 2 introduces the experimental setup and methods employed. Section 3 presents cw lasing results in detail. In Section 4, we summarize the demonstrated achievements.

2. Experimental setup

Figure 1 shows a schematic setup of the 681-nm tapered diode laser pumped Tm:YAG and Tm:LuAG laser system. The TDL that was used in this study was grown and characterized at the facilities of Ferdinand Braun Institute and detailed information on this class of diodes

can be found in [34]. Tapered diodes of similar kind were used to pump Cr:LiSAF [35, 36], Cr:LiCAF [35], Yb:KYW [37], Yb:KGW [38] and Alexandrite [39] lasers efficiently in previous studies. The TDL cavity contains a 500 μm long ridge waveguide section and a 1.5 mm long tapered amplifier section with a flared angle of 3°, and an output aperture width of 110 μm. The rear and front facets of the TDL have reflectivities of 94% and 1%, respectively. A commercial c-mount diode fixture (ILX LDM-4409) with thermoelectric temperature control is used for housing the diode. The TDL has been operated at a holder temperature of 25 °C, and at a drive current of 2 A, to receive up to 1050 mW of output power. The diode spectrum is centered at 680 nm and has a width of about 1 nm (FWHM) at 25 °C heatsink temperature. The central emission wavelength of the TDL could be tuned by varying the heatsink temperature to match the relevant absorption peak of Tm-ions (Fig. 2). The beam propagation ratio of the diode ($1/e^2$) was measured to be 4.1 and 1.1 in the slow and fast axis, respectively. The diode power content in the central lobe was measured to be 94%. The corresponding brightness of the laser device is then around 600 mW/μm^2 which is about 2 times higher than the commercial single-mode diodes and single-emitter multimode devices in the market [40]. Representative laser efficiency curves, beam waist, far field and near field profile measurements for similar TDLs could be found in [35, 39]. We note here that it is possible to grow TDLs with brightness approaching 1000 mW/μm^2 [34]; hence, the results presented in this study are likely to be improved further by using even higher quality TDLs .

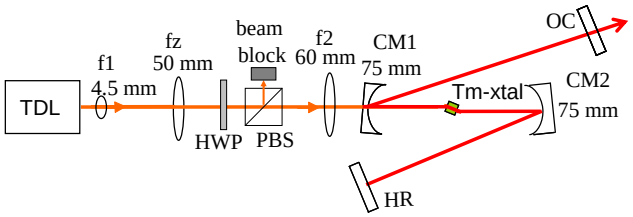

Fig. 1 Schematic of the tapered diode laser (TDL) pumped cw Tm:LuAG and Tm:YAG lasers. HWP: Half-wave plate, PBS: polarizing beam splitter cube, HR: flat high reflector, CM1-CM2: Curved cavity high reflectors, OC: output coupler.

In the laser experiments, the output of the TDL was first collected/collimated by an aspheric lens of a focal length of 4.5 mm and a numerical aperture of 0.54 (f1 in Fig 1). A second cylindrical lens of a focal length of 50 mm (fz) was used to match the divergence of the beam in different axis. Using a 60 mm focal length achromatic doublet lens (f2), the diode beam is focused inside the crystals. During the experiments the output power of the diode was kept at 1W and the amount of incident pump power on the crystal was adjusted using a polarizing beam splitter (PBS) cube and a half wave plate (HWP). Astigmatically-compensated, Z-cavities with two curved pump mirrors (CM1 and CM2, R = 75 mm), a flat end mirror (HR), and a flat output coupler (OC) were employed in the cw laser experiments. The length of the long cavity arm was adjusted to obtain a beam waist of approximately 50 μm inside the gain medium, where as the short arm length was about 25 cm long in all the experiments. 7-mm-long, 6% Tm^{3+}-doped Tm:YAG and Tm:LuAG crystals were used in the initial studies, which absorbed 97.3% and 98.1% of the incident TM polarized pump light at 681 nm, respectively. A 5-mm long 6%-Tm-doped Tm:YAG crystal was also used for investigating the effect of crystal length on laser performance (pump absorption:95.9%). Note that the absorption values stated above were measured under lasing conditions. Absorption values under non-lasing conditions were slightly lower due to pump saturation effect (~0.5% lower for the 7-mm long crystals and ~1.7% lower for the 5 mm crystal at ~800 mW incident pump power). All the crystals were 2 mm thick and mounted with indium foil in a copper holder under water cooling at 15 °C. Once lasing was obtained, the position of f1, fz, and f2 were fine adjusted to optimize the laser output power.

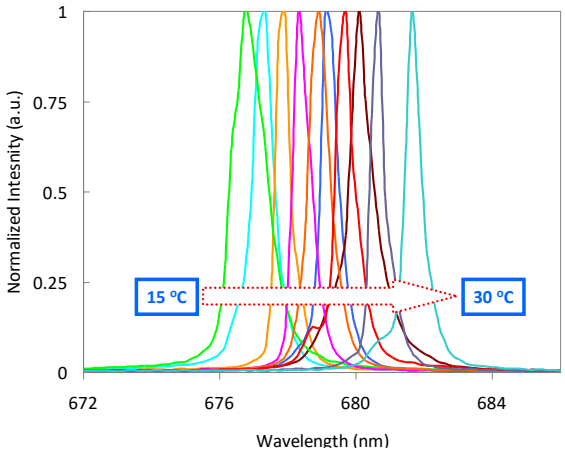

Fig. 2 Measured variation of tapered diode laser output spectrum as a function of heatsink temperature. The data is taken at an output power of 1 W.

3. Experimental results

Figure 3 shows the measured efficiency curves of the cw Tm:YAG and Tm:LuAG lasers using three different OCs with transmissions values of 1.3%, 2.7% and 4.8 %. All data in Fig. 3 were taken using the 7-mm long crystals, at a heatsink temperature of 15 °C. In both gain media, the highest laser output power was obtained using a 1.3 % OC. With this OC, the Tm:YAG laser produced 336 mW of output at an absorbed pump power level of 745 mW. The free running laser wavelength was 2019 nm (Fig. 4). The Tm:YAG laser wavelength could be tuned continuously in the 1945-2085 nm range using a 3-mm thick intracavity crystal quartz birefringent tuning element [11, 41]. Laser slope efficiency with respect to absorbed pump power was 52.7%, and the lasing threshold was around 115

mW. The laser output power fluctuations were measured to be less than 1% in a one hour measurement, clearly showing the thermal and mechanical stability of the system. Moreover, the transverse mode profile of the laser output beam was quite symmetric and circular with an M^2 below 1.1. A sample beam profile measurement is shown in Fig. 5. The data is taken with the Tm:YAG laser at the maximum output power level. The best numerical fit to the measured caustic of the focused laser output beam gave M^2 values of 1.04 and 1.09 for the horizontal and vertical axes, respectively.

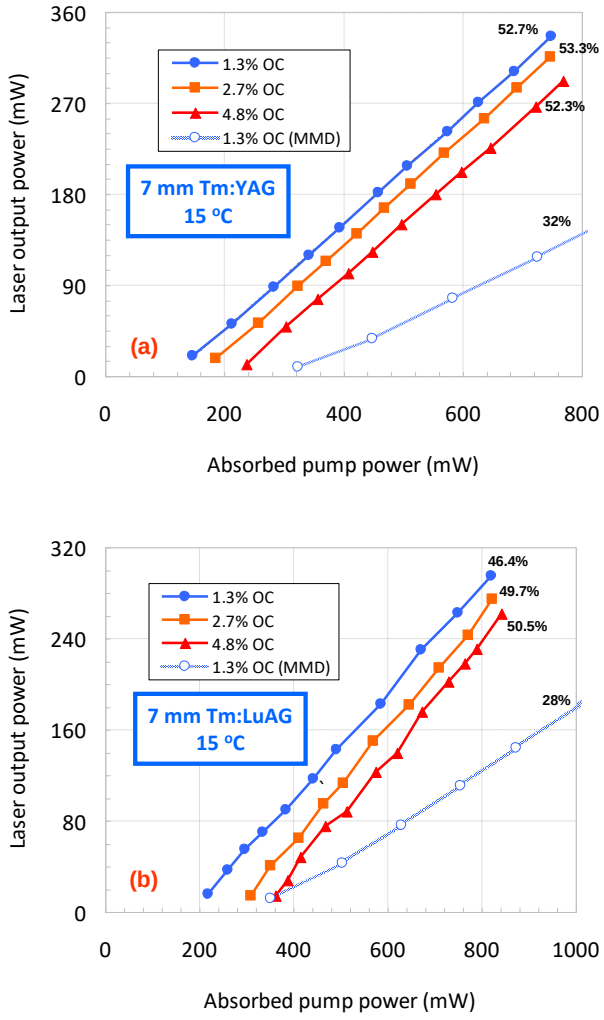

Fig. 3 Measured variation of (a) Tm:YAG and (b) Tm:LuAG laser cw output powers as a function of absorbed pump power at output coupling values of 1.3%, 2.7% and 4.8%. Results obtained with a multimode diode (MMD) is also shown for comparison purposes.

When the same system is pumped by a typical 780 nm single-emitter multimode diode (also known as broad area laser diode: BAL), with a beam propagation ratio of ~10 in the slow axis, a slope efficiency of only around 32% could be obtained under identical conditions (MMD in Fig. 3) [11]. Furthermore, the Tm:YAG laser output was also multimode, with an M^2 around 1.5 in the slow axis. It is well known that a multi-transverse mode laser output might cause beating in mode-locked regime due to interference between the lasing modes, which usually results in an unstable pulse train. Hence, the near diffraction limited output beam quality of the laser under TDL pumping demonstrates the suitability of the system for mode-locking studies as well.

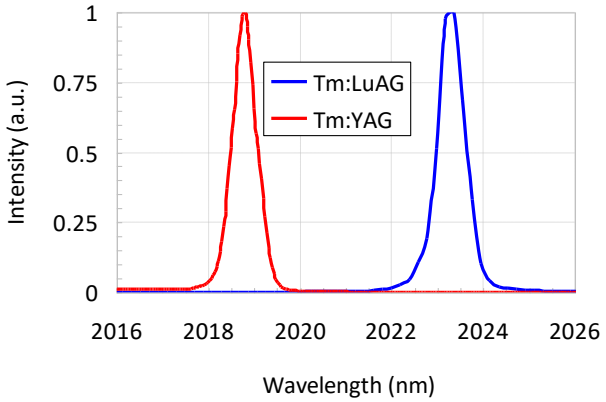

Fig. 4 Measured optical spectrum of free-running cw Tm:YAG and Tm:LuAG lasers. The measured width of spectra is limited by spectrometer resolution (0.5 nm).

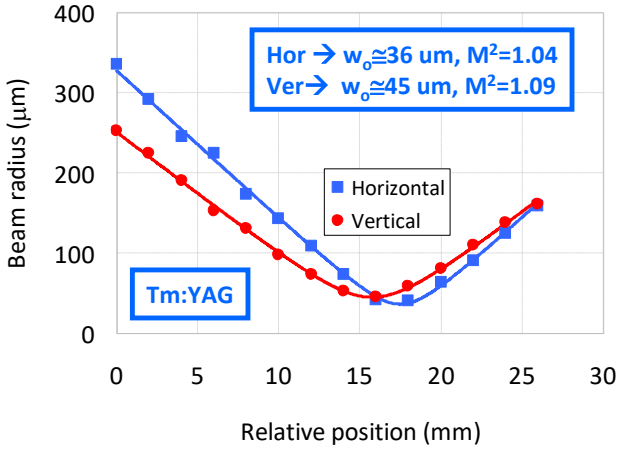

Fig. 5 Measured position dependence of the beam radius from the Tm:YAG laser near the focus of a 5 cm lens in the horizontal and vertical axes. Least-squares fitting to the experimental data gave an M^2 value of 1.04 and 1.09 for the horizontal and vertical axes, respectively.

In the case of Tm:LuAG, using the 1.3% OC, we have obtained cw output powers as high as 295 mW around 2023 nm at an absorbed pump power of 820 mW. The corresponding slope efficiency and lasing threshold were 46.4% and 185 mW, respectively. The Tm:LuAG laser wavelength could be tuned continuously in the 1940-2080 nm range using the intracavity birefringent filter. In general, as expected, the lasers slope efficiencies improved slightly with increased output coupling, and at higher output coupling we have obtained slope efficiencies up to 53.3% and 50.5 % from

the Tm:YAG and Tm:LuAG lasers, respectively (Fig. 3). Note that, as an exception, in Tm:YAG the slope efficiency obtained with the 4.8% OC is slightly lower than what is achieved using the 2.7% output coupler. We believe this slight decrease might be due to the increased rate of upconversion process at high output coupling [12].

The crystals we have used in this initial set of experiments were optimized for 785 nm pumping, and they were rather highly-doped and long (6% Tm-doping and 7-mm length). As a result, the absorption of the 681 nm pump light mostly occurred in the first few millimeters of the crystals. It is well known that, due to quasi-three-level energy band structure of the Tm-ions, gain is proportional to inversion, and a homogeneous distribution of inversion along the crystal is critical in optimizing laser performance. Moreover, if the crystal contains regions where the inversion is below a critical value, that portions of the crystal might induce self-absorption losses and deteriorate laser performance (see Fig. 1 (a) in [8]). The critical inversion level to produce positive gain depends on crystal temperature and laser wavelength. At shorter wavelengths the required critical inversion for positive gain is higher due to increased self absorption cross section value. The required critical inversion level to achieve positive gain also increases with temperature due to a decrease in effective emission cross section value and an increase in effective absorption cross section (caused by Boltzmann distribution of ions within the Stark levels at thermal equilibrium).

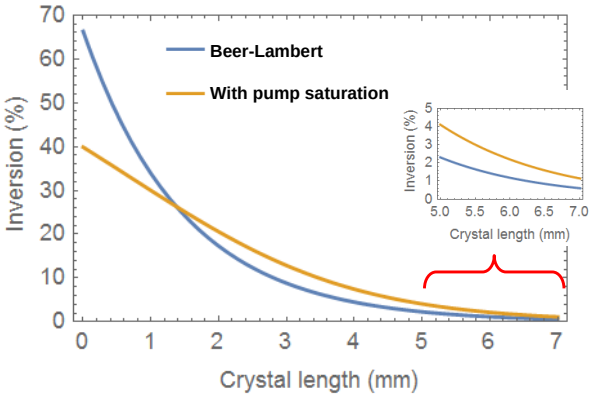

Fig. 6 Estimated variation of inversion along the 6% Tm-doped, 7-mm long Tm:YAG crystal with and without pump saturation. The inset figure shows the zoomed in inversion along the last 2 millimeter section of the crystal.

To elaborate more on this issue, Fig. 6 shows a simple estimation for the variation of inversion along the 1-W TDL pumped 7-mm long Tm:YAG crystal ignoring the transverse variation of pump beam profile. The blue curve represents the case for regular Beer-Lambert absorption profile, where as the orange curve considers the pump saturation effect [42, 43]. Note that, the case with pump saturation is calculated ignoring the intracavity circulating laser power. On the other hand, in the experiments, we have seen that the pump saturation effect almost disappears under lasing conditions. Hence, one expects the actual inversion profile to be closer to the blue curve. From Fig. 6, it is clear that the last few millimeters of the crystal do not really posses very high inversion levels, and might actually produce more harm then benefit. Specifically, we have estimated the average inversion in the last 2 millimeters of the Tm:YAG crystal to be only around 1.5 %. Based on the above analysis, we foresee that, for a 6% Tm-doped YAG sample, a 2.5-mm crystal might be a good choice in future studies (absorption is still >80% at 681 nm pumping under lasing conditions).

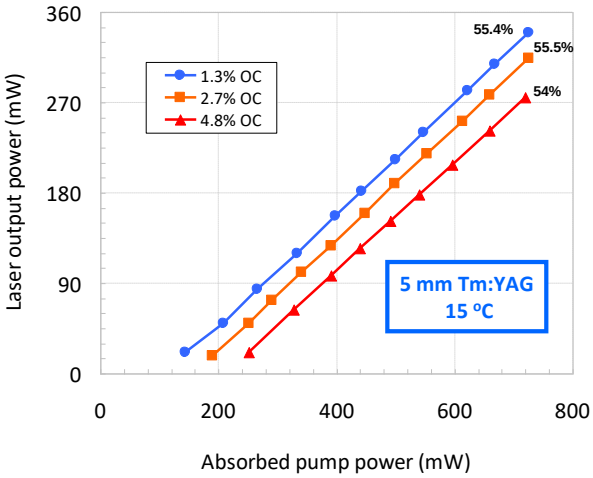

Fig. 7 Measured variation of cw output power for a Tm:YAG laser employing the 5 mm long 6% Tm-doped sample.

Unfortunately, during this study, the shortest crystal we had at hand was a 6% Tm-doped YAG with a length of 5-mm. Figure 7 shows the measured cw laser performance using this short crystal under identical conditions. Comparing Fig. 7 with Fig. 3, we clearly start to see the advantages of the shorter crystal. As an example, using the 1.3% transmitting OC, with the employment of shorter crystal, the laser slope efficiency increased from 52.7% to 55.4%. Moreover, the laser output powers obtained with the 1.3% OC increased from around 335 mW to 340 mW, despite the decrease observed in pump absorption (reduced from 745 mW to 725 mW). The observed improvement might look minor, but these results are for a central wavelength of 2019 nm. As already mentioned above, at shorter laser wavelengths, where the self absorption losses are higher, the critical inversion to achieve positive gain is larger, and hence the advantages of usage of shorter crystals will be more evident (e.g.: see Fig. 3 in [15] for the variation of self-absorption losses with wavelength). Moreover, usage of even short crystals (2.5-3 mm) could further improve the laser performance in future studies.

Material	Diode pump wavelength [nm]	Laser wavelength [nm]	Stokes limit [%]	Slope efficiency: absorbed/ incident [%]	Lasing threshold (absorbed) [W]	Photon quantum efficiency	Operating temperature [°C]	Beam quality	Ref.
4%, Tm:YAG	786	2016	39.0	65/~35	~1	1.67	8	~2.5	[19]
3%, Tm:CaF_2	792	1917	41.3	70.3/~21	~0.25	1.68	12	-	[20]
5%, Tm:KYW	802	1950	41.1	53/-	~0.15	1.29	-	-	[21]
	1750	1950	89.7	28/-	~0.3	-	-	-	
3%, Tm:YAG	785	2020	38.9	56.1/52.6	~0.75	1.44	-200	-	[44]
8% Tm:YAG	785	2012	39.0	64/-	~0.04	1.64	-	-	[45]
1%, Tm:Lu_2O_3	796	2065	38.5	46/42	~10	1.19	19	-	[12]
4%, Tm:YLF	792	1908	41.5	-/47.3	~5	1.14	15	~1.1	[46]
12%, Tm:BaY_2F_8	789	~2000	39.5	61/33	0.026	1.54	~20	-	[47]
6%, Tm:LuAG	681	2022	33.7	50.5/49.5	~0.3	1.50	15	~1.05	*
6%, Tm:YAG		2019	33.7	55.5/53.2	~0.2	1.65			

Table 1: A representative summary of diode pumped cw Tm-based solid-state laser systems in the literature.
* Indicates results obtained in this work.

Despite usage of relatively long non-optimum laser crystals, the slope efficiencies obtained in this study is among the highest slope efficiencies demonstrated from diode pumped Tm-doped solid-state laser systems. These values are also much higher than the stokes limit (34%), indicating existence of strong cross-relaxation process (with up to 1.65 photon quantum efficiency). Note that, in our study. due to large overall absorption of the crystals used, the measured slope efficiencies with respect to incident pump power is also above ~50%. Moreover, the system posses optical-to-optical and electrical-to-optical conversion efficiencies of 34% and 11%, respectively. In Table 1, we provide a representative review of diode pumped solid-state thulium laser results in literature. We believe that the high brightness and good beam quality of the 681-nm TDL that is used in this study is a significant factor for the achievement of relatively large slope efficiencies in this study. We have observed a similar advantage of TDL pumping in Cr:LiCAF lasers [35], compared to regular multimode diode pumping in our previous studies [48, 49].

In our study, the good beam quality of the TDL pump also enabled generation of near-diffraction limited laser output using a standard Z-type laser cavity. In comparison, while pumping with low-brightness pump diodes, in most cases large slope efficiencies could only be obtained from compact (5-10 cm) and simple two-mirror laser cavities, that typically also produce multimode laser output beams. However, these type of cavities are not very suitable for mode-locking and once the cavity is extended to produce mode-locking (e.g. with the insertion of an saturable Bragg reflector), the laser efficiency reduces significantly. In our case, usage of a high brightness pump source, (i) enables tight focusing of pump light into the crystal, (ii) reduces lasing threshold, (iii) provides large slope efficiencies without sacrificing from output beam quality, and (iv) enables usage of standard X or Z-cavities. We believe that, these advantages could potentially also enable efficient KLM of TDL-pumped Tm-based solid state lasers in future studies [25, 50]. We have already used a similar TDL pump sources to generate sub-15-fs long pulses from a KLM mode-locked Cr:LiSAF laser [36], showing the potential of TDLs in KLM. We believe that, if TDL pumped KLM Tm-based solid-state lasers could be developed, such low-cost, compact and simple femtosecond oscillators might become efficient seed lasers for high-power Tm-based amplifier systems.

As also mentioned in the relevant discussions above, thermal effects are quite important in quasi-3-level laser systems, since thermal distribution of laser active ions within different Stark levels change the effective absorption/emission cross section values which could significantly alter laser performance. Hence, we have carefully investigated the effect of thermal loading on the laser crystals by measuring the variation of cw laser performance at various temperatures of the crystal heatsink. Figure 8 shows the measured cw laser output power versus cupper heatsink temperature for the Tm:YAG and Tm:LuAG lasers, at an absorbed pump power level of 800 mW. For all cases the achievable laser output power levels steadily decreased with increasing crystal heat sink temperature. The results clearly show the positive effect of usage of lower crystal temperatures on laser performance in both gain media. Note that the decrease in laser performance is worse for the 7 mm long Tm:YAG compared to the 5 mm long sample. As also discussed above, the last 2 mm section of the sample could not reach the required critical inversion level at elevated temperatures (the minimum inversion level required to provide positive gain increases with temperature). As a result, the degradation of laser power with temperature is more significant in the longer sample.

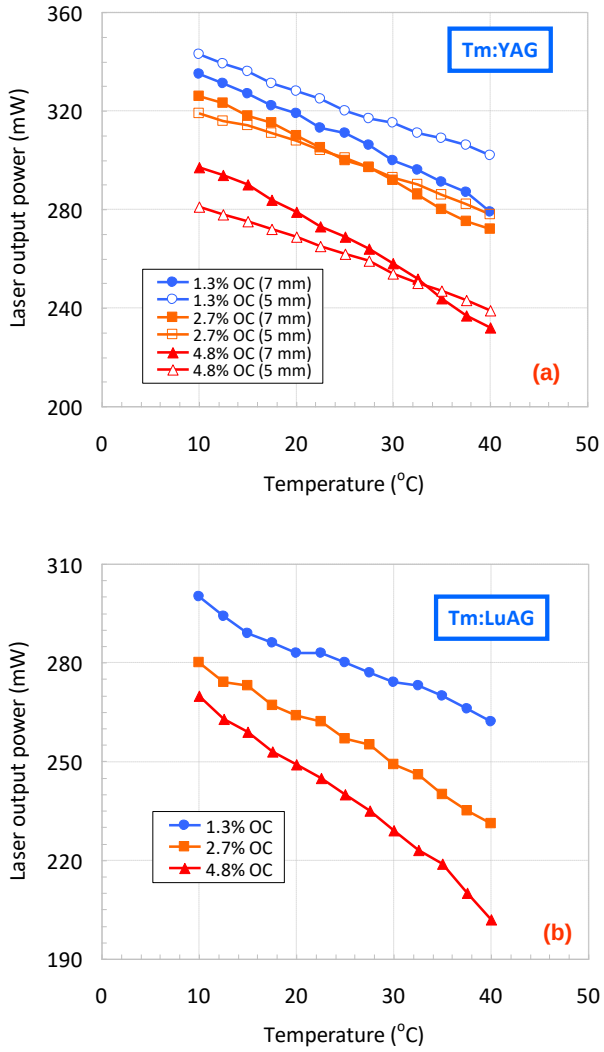

Fig. 8 (a) Tm:YAG and (b) Tm:LuAG laser cw output powers as a function of crystal heatsink temperature at output coupling values of 1.3%, 2.7% and 4.8%. The data is taken at an incident pump power of around 800 mW.

For a better understanding of the effect of crystal heatsink temperature on laser performance, Fig. 9 shows the measured variation of laser slope efficiency and lasing threshold with temperature for the 5 and 7 mm long Tm:YAG crystals at an output coupling ratio of 1.3%. Fig. 9 clearly shows that, as the temperature increases, the minimum pump power to acquire lasing increases. Moreover, the laser slope efficiency also decreases monotonically with increasing temperature. These observations are in strong agreement with previous results in literature, and could easily be understood via considering the quasi 3-level energy structure of the Tm-ion [44, 51]. As an example, a 2-fold reduction in lasing threshold and a 1.5-fold improvement in laser slope efficiency was observed in [51] when the crystal holder temperature of a diode pumped Tm:YAG laser is reduced from 20 °C to -20 °C. Coolant temperatures of -10 °C [52], 3 °C [53] and 8 °C [6, 19, 54] were also used in earlier diode pumped Tm-based solid-state laser studies. Basically, minimization of crystal heatsink temperature reduces self absorption losses via reducing the population in the lower lying laser level (highest Stark level of $^3H_6$) [44, 51]. In other words, the effective absorption cross section at the lasing wavelength reduces with temperature, which reduces self-absorption losses. Note that lower heatsink temperatures also increases the effective emission cross section values, because the ion population in the laser active Stark level of $^3F_4$ increases with decreasing temperature (2 µm lasing is generated from the transition of the lower Stark level of $^3F_4$ to the higher Stark level of $^3H_6$, see Fig. 5 in [51]). Despite the advantage of cooling, in our regular experiments, we have chosen to operate the laser at the heat sink temperature of 15 °C. This was to prevent condensation of water vapor onto the laser gain media, which could result in permanent damage to the crystal surface in long term operation. Basically, operating above the dew point simplifies the setup and minimizes the risk of crystal damage at the expense of reduced laser performance.

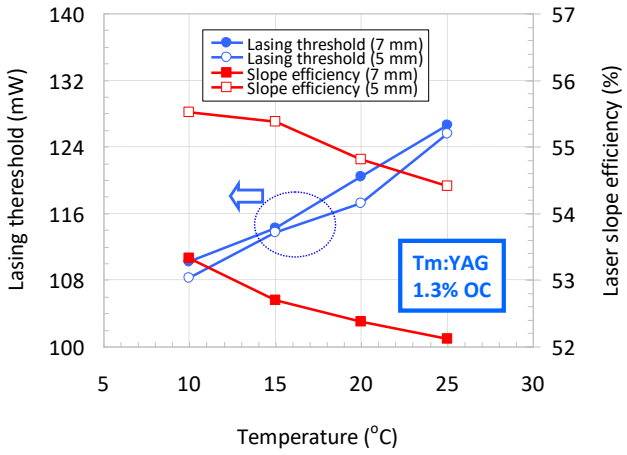

Fig. 9 Measured variation of cw lasing threshed and cw laser slope efficiency with heatsink temperature. The data is taken using the 1.3% transmitting output coupler.

4. Conclusion

In this study, we have shown that, Tm-based lasers could be effectively pumped by visible red-diodes around 680 nm. A high-brightness single-emitter tapered diode laser emitting 1-W of pump power has been used in pumping Tm:YAG and Tm:LuAG crystals. Continuous-wave output powers above 250 mW and slope efficiencies exceeding 50% could be achieved from both gain media at room temperature. The laser system provides a near diffraction limited output. The output power levels obtained in this study was limited by the available pump power from the single TDL pump source. The power levels could be further scaled up by pumping the systems with more than one tapered diode [35], by using coherently combined

pump sources [55, 56], or by employing fiber coupled diode array systems.

Acknowledgements

This work was supported in part by the Scientific and Technological Research Council of Turkey (TUBİTAK) under grant 115F053.

References

1. C. T. Wu, Y. L. Ju, F. Chen, and G. Y. Jin, "Research on 2-mu m solid-state lasers," Laser Physics **22**, 635-647 (2012).
2. B. M. Walsh, "Review of Tm and Ho materials; spectroscopy and lasers," Laser Physics **19**, 855-866 (2009).
3. T. Bilici, S. Mutlu, H. Kalaycioglu, A. Kurt, A. Sennaroglu, and M. Gulsoy, "Development of a thulium (Tm:YAP) laser system for brain tissue ablation," Lasers in Medical Science **26**, 699-706 (2011).
4. K. Murari, H. Cankaya, P. Kroetz, G. Cirmi, P. Li, A. Ruehl, I. Hartl, and F. X. Kartner, "Intracavity gain shaping in millijoule-level, high gain Ho:YLF regenerative amplifiers," Opt. Lett. **41**, 1114-1117 (2016).
5. T. Feng, K. Yang, J. Zhao, S. Zhao, W. Qiao, T. Li, T. Dekorsy, J. He, L. Zheng, Q. Wang, X. Xu, L. Su, and J. Xu, "1.21 W passively mode-locked Tm:LuAG laser," Opt. Express **23**, 11819-11825 (2015).
6. C. L. Wang, Y. X. Niu, S. F. Du, C. Zhang, Z. C. Wang, F. Q. Li, J. L. Xu, Y. Bo, Q. J. Peng, D. F. Cui, J. Y. Zhang, and Z. Y. Xu, "High-power diode-side-pumped rod Tm:YAG laser at 2.07 mu m," Appl. Opt. **52**, 7494-7497 (2013).
7. P. Gao, H. Z. Huang, X. H. Wang, H. G. Liu, J. H. Huang, W. Weng, S. T. Dai, J. H. Li, and W. X. Lin, "Passively Q-switched solid-state Tm:YAG laser using topological insulator Bi2Te3 as a saturable absorber," Appl. Opt. **57**, 2020-2024 (2018).
8. A. Gluth, Y. C. Wang, V. Petrov, J. Paajaste, S. Suomalainen, A. Harkonen, M. Guina, G. Steinmeyer, X. Mateos, S. Veronesi, M. Tonelli, J. Li, Y. B. Pan, J. K. Guo, and U. Griebner, "GaSb-based SESAM mode-locked Tm:YAG ceramic laser at 2 mu m," Opt. Express **23**, 1361-1369 (2015).
9. C. Luan, K. Yang, J. Zhao, S. Zhao, T. Li, H. Zhang, J. He, L. Song, T. Dekorsy, M. Guina, and L. Zheng, "Diode-pumped mode-locked Tm:LuAG laser at 2 mu m based on GaSb-SESAM," Opt. Lett. **42**, 839-842 (2017).
10. C. Li, J. Song, D. Y. Shen, N. S. Kim, K. Ueda, Y. J. Huo, S. F. He, and Y. H. Cao, "Diode-pumped high-efficiency Tm : YAG lasers," Opt. Express **4**, 12-18 (1999).
11. E. Beyatli, and U. Demirbas, "Widely tunable dual-wavelength operation of Tm:YLF, Tm:LuAG, and Tm:YAG lasers using off-surface optic axis birefringent filters," Appl. Opt. **57**, 6679-6686 (2018).
12. P. Koopmann, S. Lamrini, K. Scholle, P. Fuhrberg, K. Petermann, and G. Huber, "Efficient diode-pumped laser operation of Tm:Lu2O3 around 2 mu m," Opt. Lett. **36**, 948-950 (2011).
13. E. Beyatli, S. Naghizadeh, A. Kurt, and A. Sennaroglu, "Low-cost low-threshold diode end-pumped Tm:YAG laser at 2.016 mu m," Appl. Phys. B **109**, 221-225 (2012).
14. J. W. Zhang, F. Schulze, K. F. Mak, V. Pervak, D. Bauer, D. Sutter, and O. Pronin, "High-Power, High-Efficiency Tm:YAG and Ho:YAG Thin-Disk Lasers," Laser & Photonics Reviews **12** (2018).
15. R. C. Stoneman, and L. Esterowitz, "Efficient, broadly tunable, laser-pumped Tm:YAG and Tm:YSGG cw lasers," Opt. Lett. **15**, 486-488 (1990).
16. J. Korner, T. Luhder, J. Reiter, I. Uschman, H. Marschner, V. Jambunathan, A. Lucianetti, T. Mocek, J. Hein, and M. C. Kaluza, "Spectroscopic investigations of thulium doped YAG and YAP crystals between 77 K and 300 K for short-wavelength infrared lasers," J. Lumin. **202**, 427-437 (2018).
17. V. Sudesh, and E. M. Goldys, "Spectroscopic properties of thulium-doped crystalline materials including a novel host, $La_2Be_2O_5$: a comparative study," J. Opt. Soc. Amer. B **17**, 1068-1076 (2000).
18. X. D. Xu, X. D. Wang, Z. F. Lin, Y. Cheng, D. Z. Li, S. S. Cheng, F. Wu, Z. W. Zhao, C. Q. Gao, M. W. Gao, and J. Xu, "Crystal growth, spectroscopic and laser properties of Tm:LuAG crystal," Laser Physics **19**, 2140-2143 (2009).
19. W. L. Gao, J. Ma, G. Q. Xie, J. Zhang, D. W. Luo, H. Yang, D. Y. Tang, J. Ma, P. Yuan, and L. J. Qian, "Highly efficient 2 mu m Tm:YAG ceramic laser," Opt. Lett. **37**, 1076-1078 (2012).
20. J. J. Liu, C. Zhang, Z. Zhang, J. Y. Wang, X. W. Fan, J. Liu, and L. B. Su, "1886-nm mode-locked and wavelength tunable Tm-doped CaF2 lasers," Opt. Lett. **44**, 134-137 (2019).
21. A. E. Troshin, V. E. Kisel, A. S. Yasukevich, N. V. Kuleshov, A. A. Pavlyuk, E. B. Dunina, and A. A. Kornienko, "Spectroscopy and laser properties of Tm3+: KY(WO4)(2) crystal," Appl. Phys. B **86**, 287-292 (2007).
22. F. Cornacchia, A. Di Lieto, P. Maroni, P. Minguzzi, A. Toncelli, M. Tonelli, E. Sorokin, and I. Sorokina, "A cw room-temperature Ho,Tm : YLF laser pumped at 1.682 um," Appl. Phys. B **73**, 191-194 (2001).
23. Y. L. Kalachev, V. A. Mihailov, V. V. Podreshetnikov, and I. A. Shcherbakov, "The study of a Tm:YLF laser pumped by a Raman shifted Erbium fiber laser at 1678 nm," Opt. Comm. **284**, 3357-3360 (2011).
24. Y. Wang, D. Y. Shen, H. Chen, J. Zhang, X. P. Qin, D. Y. Tang, X. F. Yang, and T. Zhao, "Highly efficient Tm:YAG ceramic laser resonantly pumped at 1617 nm," Opt. Lett. **36**, 4485-4487 (2011).
25. M. Tokurakawa, E. Fujita, and C. Krankel, "Kerr-lens mode-locked Tm3+:Sc2O3 single-crystal laser in-band pumped by an Er:Yb fiber MOPA at 1611 nm," Opt. Lett. **42**, 3185-3188 (2017).
26. Q. Ke, S. Y. Tan, S. T. Liu, D. Lu, R. K. Zhang, W. Wang, and C. Ji, "Fabrication and optimization of 1.55-mu m InGaAsP/InP high-power semiconductor diode laser," Journal of Semiconductors **36** (2015).
27. M. Guina, A. Rantamaki, and A. Harkonen, "Optically pumped VECSELs: review of technology and progress," Journal of Physics D-Applied Physics **50** (2017).
28. F. Wu, W. C. Yao, H. T. Xia, Q. Y. Liu, M. M. Ding, Y. G. Zhao, W. Zhou, X. D. Xu, and D. Y. Shen, "Highly efficient continuous-wave and Q-switched Tm:CaGdAlO4 laser at 2 mu m," Optical Materials Express **7**, 1289-1294 (2017).
29. D. Creeden, B. R. Johnson, S. D. Setzler, and E. P. Chicklis, "Resonantly pumped Tm-doped fiber laser with > 90% slope efficiency," Opt. Lett. **39**, 470-473 (2014).
30. R. C. Stoneman, J. F. Pinto, L. Esterowitz, and G. H. Rosenblatt, "681-nm-pumped 2 um Tm:YAG Laser," in *LEOS*(IEEE, Boston, 1992), p. SSLT2.2.
31. U. Demirbas, "Power scaling potential of continuous-wave Cr:LiSAF and Cr:LiCAF lasers in thin-disk geometry," Appl. Opt. **57**, 10207-10217 (2018).
32. C. Y. Cho, Y. F. Chen, G. Zhang, W. D. Chen, and H. C. Liang, "Exploring the self-mode locking of the 2 mu m Tm:YAG laser with suppression of the self-pulsing dynamic," Opt. Lett. **42**, 5226-5229 (2017).
33. P. S. F. De Matos, N. U. Wetter, L. Gomes, I. M. Ranieri, and S. L. Baldochi, "A high power 2.3 mu m Yb : Tm : YLF laser diode-pumped simultaneously at 685 and 960 nm," Journal of Optics a-Pure and Applied Optics **10** (2008).
34. B. Sumpf, P. Adamiec, M. Zorn, H. Wenzel, and G. Erbert, "Nearly Diffraction Limited Tapered Lasers at 675 nm with 1 W Output Power and conversion efficiencies above 30%," IEEE Photonic. Tech. L. **22**, 266-268 (2011).
35. U. Demirbas, M. Schmalz, B. Sumpf, G. Erbert, G. S. Petrich, L. A. Kolodziejski, J. G. Fujimoto, F. X. Kärtner, and A. Leitenstorfer, "Femtosecond Cr:LiSAF and Cr:LiCAF lasers pumped by tapered diode lasers," Opt. Express **19**, 20444-20461 (2011).
36. C. Cihan, E. Beyatli, F. Canbaz, L.-J. Chen, B. Sumpf, G. Erbert, A. Leitenstorfer, F. X. Kärtner, A. Sennaroğlu, and U. Demirbas, "Gain-Matched Output Couplers for Efficient Kerr-Lens Mode-Locking of Low-Cost and High Peak-Power Cr: LiSAF Lasers," IEEE J. Sel. Top. Quantum Electron. **21** (2015).
37. P. Klopp, V. Petrov, U. Griebner, and G. Erbert, "Passively mode-locked Yb:KYW laser pumped by a tapered diode laser," Opt. Express **10**, 108-113 (2002).
38. S. Pekarek, A. Klenner, T. Südmeyer, C. Fiebig, K. Paschke, G. Erbert, and U. Keller, "Femtosecond diode-pumped solid-state laser with a repetition rate of 4.8 GHz," Opt. Express **20**, 4248-4253 (2012).
39. E. Beyatli, I. Baali, B. Sumpf, G. Erbert, A. Leitenstorfer, A. Sennaroglu, and U. Demirbas, "Tapered diode-pumped continuous-wave alexandrite laser," J Opt Soc Am B **30**, 3184-3192 (2013).
40. H. Wenzel, B. Sumpf, and G. Erbert, "High-brightness diode lasers," Comptes Rendus Physique **4**, 649-661 (2003).
41. U. Demirbas, "Off-surface optic axis birefringent filters for smooth tuning of broadband lasers," Appl. Opt. **56**, 7815-7825 (2017).
42. Y. Sato, and T. Taira, "Saturation factors of pump absorption in solid-state lasers," IEEE J. Quantum Electron. **40**, 270-280 (2004).
43. A. Sennaroglu, U. Demirbas, S. Ozharar, and F. Yaman, "Accurate determination of saturation parameters for Cr4+-doped solid-state saturable absorbers," J Opt Soc Am B **23**, 241-249 (2006).

44. J. G. Li, T. Yan, J. T. Liang, and J. H. Cai, "Measurement of output characteristics of Tm:YAG laser at 25-300 K," Opt. Comm. **334**, 118-121 (2015).
45. A. Rameix, C. Borel, B. Chambaz, B. Ferrand, D. P. Shepherd, T. J. Warburton, D. C. Hanna, and A. C. Tropper, "An efficient, diode-pumped, 2 mu m Tm:YAG waveguide laser," Opt. Comm. **142**, 239-243 (1997).
46. X. M. Duan, B. Q. Yao, Y. J. Zhang, C. W. Song, L. L. Zheng, Y. L. Ju, and Y. Z. Wang, "Diode-pumped high efficient Tm : YLF laser output at 1908 nm with near-diffraction limited beam quality," Laser Physics Letters **5**, 347-349 (2008).
47. F. Cornacchia, D. Parisi, C. Bernardini, A. Toncelli, and M. Tonelli, "Efficient, diode-pumped Tm3+: BaY2(F8) vibronic laser," Opt. Express **12**, 1982-1989 (2004).
48. U. Demirbas, A. Sennaroglu, F. X. Kartner, and J. G. Fujimoto, "Comparative investigation of diode pumping for continuous-wave and mode-locked Cr3+ : LiCAF lasers," J Opt Soc Am B **26**, 64-79 (2009).
49. U. Demirbas, A. Sennaroglu, A. Benedick, A. Siddiqui, F. X. Kärtner, and J. G. Fujimoto, "Diode-pumped, high-average power femtosecond Cr^{+3}:LiCAF laser," Opt. Lett. **32**, 3309-3311 (2007).
50. F. Canbaz, I. Yorulmaz, and A. Sennaroglu, "Kerr-lens mode-locked 2.3-mu m Tm3+:YLF laser as a source of femtosecond pulses in the mid-infrared," Opt. Lett. **42**, 3964-3967 (2017).
51. C. Li, J. Song, D. Shen, N. S. Kim, and K.-i. Ueda, "Diode-pumped high-effiency Tm:YAG lasers," Opt. Express **4**, 12-18 (1999).
52. K. S. Lai, W. J. Xie, R. F. Wu, Y. L. Lim, E. Lau, L. Chia, and P. B. Phua, "A 150W 2-micron diode-pumped Tm:YAG laser," in *Advanced Solid State Lasers* (Québec City Canada, 2002), p. WE6.
53. E. C. Honea, R. J. Beach, S. B. Sutton, J. A. Speth, S. C. Mitchell, J. A. Skidmore, M. A. Emanuel, and S. A. Payne, "115-W Tm:YAG diode-pumped solid-state laser," IEEE J. Quantum Electron. **33**, 1592-1600 (1997).
54. D. Cao, Q. Peng, S. Du, J. Xu, Y. Guo, J. Yang, Y. Bo, J. Zhang, D. Cui, and Z. Xu, "A 200 W diode-side-pumped CW 2 mu m Tm:YAG laser with water cooling at 8 degrees C," Appl. Phys. B **103**, 83-88 (2011).
55. T. Y. Fan, "Laser beam combining for high-power, high-radiance sources," IEEE J. Sel. Top. Quantum Electron. **11**, 567-577 (2005).
56. P. Albrodt, M. T. Jamal, A. K. Hansen, O. B. Jensen, G. Blume, K. Paschke, P. Crump, P. Georges, and G. Lucas-Leclin, "Coherent combining of high brightness tapered amplifiers for efficient non-linear conversion," Opt. Express **27**, 928-937 (2019).